Endocycling in the adult Drosophila accessory gland

Allison M. Box[1], Samuel Jaimian Church[1], David Hayes[1], Shyama Nandakumar[1], Russell S. Taichman[2], and Laura Buttitta[1]

[1] Department of Molecular, Cellular and Developmental Biology, University of Michigan, Ann Arbor, MI 48109, USA

[2] Department of Periodontics and Oral Medicine, University of Michigan School of Dentistry, Ann Arbor, MI 48109, USA

* Author for correspondence: buttitta@umich.edu

Abstract

The *Drosophila melanogaster* accessory gland is a functional analog of the mammalian prostate made up of two secretory epithelial cell types, termed main and secondary cells. This tissue is responsible for making and secreting seminal fluid proteins and other molecules that contribute to successful reproduction. Here, we show that similar to the mammalian prostate, this tissue grows with age. We find that the adult accessory gland grows in part via endocycles to increase DNA content and cell size. The differentiated, bi-nucleated main cells remain poised to endocycle in the adult gland, and tissue damage or upregulation of signals that promote growth are sufficient to trigger dramatic endocycling leading to increases in cell size and ploidy, independent of mating status. Our data establishes that the adult accessory gland is not quiescent, but instead uses endocycles to maintain accessory gland function throughout the fruit fly's lifespan.

Introduction

The *Drosophila* accessory gland is functionally analogous to the mammalian prostate. This tissue is an essential component of the male reproductive system and is responsible for making and secreting seminal fluid proteins, sex peptides, and anti-microbial proteins that are transferred to the female upon mating (Ravi Ram, Ji, and Wolfner 2005; Qazi and Wolfner 2003; Lung, Kuo, and Wolfner 2001; Adams and Wolfner 2007; Heifetz et al. 2005). The accessory gland is a mono-layered, secretory tissue comprised of a single layer of epithelial cells that envelops a large lumen and is surrounded by a muscle layer (Susic-Jung et al. 2012; Bairati 1968). Each lobe of the accessory gland consists of approximately 1,000 epithelial cells, which are made up of two cell types: main cells and secondary cells (Bairati 1968). Main cells are the smaller of the two types and are hexagonal in shape. These cells make up a majority of the gland and are located mostly in the proximal and medial portions of the lobes. Secondary cells are larger, more luminal cells that are located at the distal tip of the lobes. There are approximately 40-60 secondary cells in each lobe, with the rest of the cells (~940-960 cells) being main cells. Each accessory gland cell type has a distinct but partially overlapping secretory protein profile and both cell types play an important role in fecundity (Bertram et al. 1992; Sitnik et al. 2016).

In late larval stages, FGF signaling drives recruitment of mesodermal cells to the genital disc. These cells undergo a mesenchymal to epithelial transition and give rise to the precursors for the accessory glands and seminal vesicles (Ahmad and Baker 2002). During early metamorphosis, the accessory gland progenitors increase in number by standard mitotic cell cycles. Approximately 50-55 hours after pupa formation, the cells of the developing accessory gland arrest proliferation and synchronously enter a truncated variant cell cycle, in which nuclear division occurs but cytokinesis does not, resulting in the bi-nucleation of the epithelial cells of the accessory gland. Approximately 10 hours later, the cells enter an additional synchronized endocycle, increasing their DNA content without mitosis. This results in ~1,000 binucleate cells containing two 4N nuclei. After this endocycle, the cells of the accessory gland exit the cell cycle (Taniguchi et al. 2014) and are thought to remain quiescent in the adult (Leiblich et al. 2012).

The presence of synchronized cycling and multiple types of variant cell cycles suggests that the accessory gland has complex and intricate cell cycle regulation that has yet to be uncovered. Until recently it was thought the adult tissue was non-cycling, however a recent preprint describes secondary cell endoreplication that occurs in a mating dependent manner (Leiblich et al. n.d.). We examined endoreplication in the adult accessory gland from eclosion and find many examples of endoreplication in main cells, independent of mating status. Tissue damage or induction of growth signals are also sufficient to trigger a dramatic increase of endocycling in the differentiated adult tissue, even in the absence of mating. Our work establishes that the adult accessory gland main cells are binucleate, polyploid cells that remain poised to endocycle to maintain gland function throughout the fruit fly's lifespan.

The adult accessory gland grows via endoreplication, independent of mating status, under normal physiological conditions throughout lifespan.

Like the mammalian prostate, the *Drosophila* accessory gland (AG) grows with age. AGs from virgin males undergo a period of rapid growth from the day of eclosion to day 10 post eclosion (Fig 1A), and continues to grow, albeit at a lesser rate throughout adulthood (Fig 1B). While some AG growth in early adulthood can be attributed to the production and secretion of sex peptides which expands the lumen of the gland, we hypothesized that changes in cell number or cell size may also contribute to gland growth. To address whether a mitotic population exists in the AG, we stained the adult AG for the mitotic marker, phospho-histone H3 (PH3), at various timepoints throughout the male lifespan. In sum, over 100 AGs, of various ages with and without mating, were negative for PH3 staining (data not shown). We therefore postulated that under normal physiological conditions, gland growth is due to changes in cell size rather than cell number.

We next measured cell size for the major population of cells in the AG, the main cells. Antibody staining for the septate junction protein Discs large (Dlg) was used for all cell size measurements. Because of the apical localization of Dlg, cell size measurements reported here are not the full volume of a cell, but rather a measurement of the apical area. In virgin males, main cell size increases with age throughout lifespan (Fig 1C), and the variation in main cell size throughout the gland also increases with age. Previous studies have established that cell size often scales with nuclear size (Orr-Weaver 2015). We therefore next measured nuclear size in main cells across lifespan and found that nuclear area and variance also tracks with the increases in main cell size with age (FIG 1C). Together, our data shows a correlation between increased AG size, main cell size, and main cell nuclear area throughout the lifespan of the fly (Fig 1).

Many tissues undergo a variant cell cycle called an endocycle in order to increase tissue size under normal physiological conditions (Orr-Weaver 2015; Edgar, Zielke, and Gutierrez 2014). Endocycling occurs when cells cycle through G/S phases without entering an M phase, thereby increasing DNA content resulting in polyploidy. Increased ploidy can contribute to increased biosynthesis, as is the case with *Drosophila* nurse cells (Orr-Weaver 2015; Inge Øvrebø and Edgar 2018). In this context, endocycling may be essential for optimal function of the adult AG, which is highly secretory and responsible for making large

amounts of accessory gland specific proteins and other molecules for transfer to the female upon mating (Prince et al. 2019; Wilson et al. 2017). Because cell size scales with DNA content in *Drosophila* endocycling cells (Von Stetina et al. 2018), we next examined whether DNA replication occurs in the main cells of this tissue. We examined the AG immediately after eclosion, before the males eat or mate. To label S-phases we incubated tissues with EdU for one hour, since we found labeling by feeding to be ineffective at this stage. Upon a one-hour EdU incubation, we observed extensive nuclear labeling in most main cells, demonstrating that the adult AG undergoes a very early wave of endocycling in main cells. We hypothesize that the burst of widespread EdU incorporation that we see results from a relatively synchronous round of endoreplication occurring within the first few hours after eclosion that likely supports the extensive growth and maturation of this gland during the first few days of adulthood (Koppik et al. 2018). We believe this round of endoreplication in the AG has been previously missed due to the use of feeding-based labeling assays, since adult male flies do not eat for 4.5-5 hours post eclosion (data not shown).

To assess endocycling in aging adults, we performed EdU incorporation experiments by feeding adult male flies an EdU/sucrose mixture for 10 day windows at different time points throughout their lifespan. This longer-term EdU labeling allowed us to visualize slow or rare DNA replication events in the adult AG. We found that the main cells of the AG continue to endocycle throughout the lifespan of the fly up to 50 days of age (Fig 1D) under both starved and fed conditions (fed data not shown). We only very rarely observed secondary cells labeled with EdU, and this was independent of mating status (Fig 1E,F). We conclude that adult AG main cells undergo endocycling throughout the *Drosophila* lifespan under normal, physiological conditions with and without mating.

Cell cycle degradation machinery oscillates in the adult accessory gland

Our pulsed and long-term EdU labeling approach provides a static picture of S-phase but does not reveal cell cycle transitions and oscillations in real-time. To address this, we used Fly FUCCI cell cycle reporters to examine the oscillations of the cell cycle degradation machinery in the AG (Zielke et al. 2014). We used *Paired-Gal4* (*Prd-Gal4*), a driver that has been established to express in main and secondary cells, to drive expression of the cell

cycle protein degrons mRFP1-CycB$_{1-266}$, to assay APC/C^{Cdh1} activity, and GFP-E2F1$_{1-230}$, to assay CRL4(Cdt2) activity. (Fig 2A). We find that more than 24h after eclosion, the majority of main and secondary cells have low levels of mRFP1-CycB$_{1-266}$ indicating most cells are normally in a Gap phase with high APC/C^{Cdh1} activity, except for a small subset of main and very rare secondary cells where high mRFP1-CycB$_{1-266}$ indicates low APC/C^{Cdh1} activity. The low APC/C^{Cdh1} activity in endocycles results from transient high CycE/Cdk2 which also triggers S-phase, suggesting these cells have recently undergone DNA synthesis (Narbonne-Reveau et al. 2008; Zielke et al. 2008). The relatively low numbers of these cells at individual fixed timepoints roughly agrees with the number of S-phases we observe in our longer term EdU labeling. The GFP-E2F1$_{1-230}$ reporter indicates CRL4(Cdt2) activity which is normally high during S-phase and low during Gap phase. The high levels of GFP-E2F1$_{1-230}$ throughout the gland verifies that most cells are in a Gap phase where CRL4(Cdt2) activity is low, but a number of main cells and rare secondary cells show high CRL4(Cdt2) activity, consistent with transitions through S-phase. This Fly FUCCI signature is similar to other endocycling cells, such as the intestinal enterocytes (Zielke et al. 2014).

We verified the Fly FUCCI results by using the RGB cell cycle sensor as an additional tool to track cell cycle degradation machinery activity (Fig 2B). The RGB cell cycle sensor uses the Gal4-UAS system to drive overexpression of cell cycle protein degrons nlsCycB$^{1-96}$-nlsCycB$^{1-285}$-tdTomato, to assay APC/C activity, and nlsCdt1$^{1-101}$-EBFP2, to assay CRL4(Cdt2) activity, as well as a full length EGFP-PCNA to visualize early S Phase (Handke et al. 2014). While similar in concept to Fly FUCCI, a few notable differences include: a different length fragment of CycB, the use of nlsCdt1$^{1-101}$ instead of E2F1$_{1-230}$, and the expression of all 3 fluorescent reporters from a single transcript. Consistent with our findings using Fly FUCCI, we see that generally APC/C activity is high and CRL4(Cdt2) activity is low throughout the gland with only a small subset of main cells exhibiting EGFP-PCNA foci indicative of S-Phase. Importantly, oscillations of the cell cycle degrons occur at the distal tip where main and secondary cells are located, as well as mid-lobe where there are no secondary cells (Fig 2B).

Since we rarely observe S-phases in secondary cells, we looked more carefully into differences between cell cycle reporters in main and secondary cells. We noted obvious differences in the levels of GFP-E2F1$_{1-230}$ and nlsCdt1$^{1-101}$-EBFP2 (Fig 2C) between

secondary and main cells. Specifically, GFP-E2F1$_{1-230}$ levels appear stabilized in secondary cells while nlsCdt1$^{1-101}$-EBFP2 seems to be highly de-stabilized. This is surprising as both of these fragments contain a PIP-box degradation sequence and would be expected to follow similar degradation patterns during S-phase. The stabilization of GFP-E2F1$_{1-230}$ in secondary cells suggests that S-phase coupled CRL4(Cdt2) activity is lower in secondary cells than main cells. This is consistent with our finding that we very rarely see EdU labeled S-phases or PCNA-GFP foci in secondary cells. However the lower levels of nlsCdt1$^{1-101}$-EBFP2 in the secondary cells suggests that Cdt1 levels in secondary cells may be controlled by an additional degradation complex. Mammalian Cdt1 is also regulated via a Cdk phosphodegron recognized by the SCF^{Skp2} complex (Pozo and Cook 2016), and we find that a potential Cdk phosphorylation site and potential Skp2 degradation motif is intact in the nlsCdt1$^{1-101}$-EBFP2 reporter (Supp. Fig. 1). We propose that SCF^{Skp2} may play a role in keeping Cdt1 levels low in adult *Drosophila* secondary cells, thereby limiting replication licensing in this cell type, leading to the very rare endocycles we observe (see discussion for further detail).

One caveat of the cell cycle reporters is their dependence on the Gal4-UAS system for ectopic expression of fluorescently tagged degrons. We therefore confirmed our observations using an endogenously tagged PCNA (PCNA::GFP) to confirm the presence of PCNA protein and to use GFP expression as a real-time read out of S-phase activity in this tissue (Blythe and Wieschaus 2016). PCNA::GFP is present in nearly every main cell on the day of eclosion (Fig 2D, top panel). Consistent with our EdU labeling on the day of eclosion and fly FUCCI data, we see lower levels of PCNA::GFP in secondary cells than main cells, suggesting that these cells are refractory to S-phase during this early wave of endocycling. In older AGs PCNA::GFP expression in main cells is greatly reduced (Fig 2D, bottom panel), however we find a small subset of main cells that are PCNA::GFP positive and we did not observe any endogenous PCNA::GFP expression in secondary cells, even under mated conditions. We conclude that upon eclosion, a wave of endocycling occurs in most, if not all, main cells of the AG leading to dramatic growth and an increase in main cell ploidy in the first day. After that, we find low, but persistent endocycling in several main cells throughout the gland, potentially to maintain tissue homeostasis throughout adulthood, accompanied by very rare (only 2 observed) endocycles in secondary cells.

The adult accessory gland exhibits compensatory cellular hypertrophy in response to damage

The adult AG exhibits a low level of endocycling for normal tissue homeostasis. Due to the importance of the AG for successful reproduction, we wondered whether this tissue can respond to damage and how damage may affect cell cycling. Upon injury, tissues that have a mitotic population increase cell division to allow for regeneration after damage; however, we do not observe an obvious mitotic population in the adult AG. One mechanism of tissue regeneration in post-mitotic tissues is compensatory cellular hypertrophy (CCH), an increase in cell size that stems from endoreplication (Tamori and Deng 2013a). Similarly other postmitotic tissues exhibit wound induced polyploidization (WIP), which can be a result of cell fusion, but is also driven in part by endocycling (Losick, Fox, and Spradling 2013; Losick, Jun, and Spradling 2016). Because the adult AG maintains the capacity to endocycle, we examined whether this tissue may exhibit features of CCH and/or WIP in response to damage.

We used the DEMISE system to induce cell death in the AG. The DEMISE system uses a heat-shock-flippase (*hs-Flp*) with a UAS-driven "flipout cassette" to induce controlled Reaper expression, driving caspase dependent apoptosis (Cohen et al. 2018). We find that the DEMISE system induces apoptosis in the AG and can be used to study the response to damage in the adult AG (Fig 3). We used three experimental procedures with DEMISE to induce damage and allow for varying levels of recovery (Fig 3A). While DEMISE contains a *hs-Flp* to induce damage, we quickly realized that all versions of the system we tested lead to leaky expression of the *flp* enzyme in the late pupal AG after 60h APF at room temperature. Therefore, all DEMISE experiments described in this paper use the leaky expression at late pupal stages to induce damage. When we dissect AGs expressing DEMISE on the day of eclosion (red), we find that 100% of AGs show damage in at least one lobe with the majority of samples exhibiting one lobe with more damage than the other (Fig 3F). When we dissect AGs expressing DEMISE three days post eclosion (blue), we observe that AGs have increased in size since the day of eclosion, but the tissue shows signs of continued damage (Fig 3C), with an increased percentage of animals exhibiting high levels of damage in both lobes (Fig 3F). In a third procedure, we collected animals the day of eclosion, when

100% of animals we tested exhibit damage, and immediately shifted them to 18°C for 5 days to reduce the Gal4/UAS-driven reaper expression to allow for some level of recovery. Indeed, using this protocol we observed striking recovery of gland morphology and size. By 5 days of recovery only 20% of animals show obvious AG defects, compared to 100% of animals which show damage on the day of eclosion (Fig 3D orange outline, Fig 3F). Importantly, we observed no animal lethality with these DEMISE protocols, so we are confident we are not selecting for survivors at day 5. In all experimental procedures the adult AG contained binucleated, pyknotic nuclei, indicating that Reaper induces apoptosis in AG cells after the binucleation event during development. Further, we observe binucleated pyknotic nuclei in all of our experiments, regardless of age, suggesting that Reaper continues to induce cell death in the differentiated binucleate adult tissue (Fig 3E), although at reduced levels in our recovery protocol.

The adult AG exhibits the capacity to recover in size after tissue damage. The high frequency of the single damaged lobe phenotype can be used as an in-animal control to compare the recovery response of a lobe that undergoes extensive damage to the recovery response of a lobe that undergoes much less damage. Here we show two AG lobes from the same animal after the recovery protocol (Fig 3G). The numbers of pyknotic nuclei indicate which lobe has undergone the most extensive damage. It is clear that one lobe has many more pyknotic nuclei, a greater variation in nuclear size, and cells that are much larger, consistent with CCH (Fig 3H). However, we never observe cells with more than two nuclei under any protocol, suggesting the cell fusion aspect of the WIP response is absent. We conclude that the adult AG can partially recover from cell death-induced damage via CCH.

The adult accessory gland increases endoreplication in response to tissue damage

We have shown the AG responds to cell death by increased cell size and nuclear size under our recovery protocol. We next tested whether the CCH we observe in the adult *Drosophila* AG is due to an increase in endocycling, as is described in previous work on other post-mitotic tissues (Losick, Fox, and Spradling 2013; Tamori and Deng 2013b). We coupled DEMISE induced damage with a longer recovery including EdU feeding to label cells that endocycle during recovery. Animals were raised at room temperature, collected the day of eclosion, and shifted to 18°C for 11 days and fed EdU/sucrose for the entire recovery (Fig.

4A red). We observed increased levels of endocycling throughout the tissue (Fig 4B,C), to an extent much higher than that observed under normal physiological conditions. To address whether there is a critical time window for damage induced endocycling, we performed the same recovery protocol except that animals were fed standard CM for the first 5 days, and only fed EdU/sucrose for the remaining 6 days (Fig. 4A blue). Again, we observed increased endocycling throughout the gland even after 5 days of recovery, demonstrating that increased endocycling continues and is not limited to an early acute damage response. Together, our data suggests that the adult AG is not quiescent, but instead, uses endocycles for normal tissue homeostasis and is poised to induce endocycles in response to tissue damage.

Cells of the adult accessory gland are poised to endocycle in response to growth signals

The increased endoreplication that occurs in response to damage indicates that the adult AG is poised to endocycle when given proper cues. We reasoned that activation of signals upregulated in response to wounding may induce endoreplication leading to CCH in the AG cells recovering from the DEMISE protocol. We therefore examined several factors known to promote endocycling in response to wounding.

We examined the pro-oncogenic transcription factor Myc and the Hippo signaling effector Yki, which have been shown to promote the endocycling phase of wound induced polyploidy (WIP) in drosophila epithelium (Losick, Fox, and Spradling 2013; Grendler et al. 2019; Losick, Jun, and Spradling 2016) coupled with co-expression of the E2F activator complex E2F1/DP, which is essential for endocycling (Norman Zielke et al. 2011). We also examined the effects of expressing a constitutively active form of the BMP type I receptor Thickveins (Tkv*), as BMP/Dpp signaling has been shown to promote compensatory proliferation in wounded tissues (Zhou et al. 2015) and was recently shown to promote endocycling in the AG secondary cells in response to mating (Leiblich et al., n.d.). We used the FLP-FRT system to create clones expressing these growth regulators in the adult AG (Fig 5A). In brief, this method uses a *hs-flp* to recombine FRT sites in an actin promoter-driven "flipout" (act-FRT-stop-FRT-Gal4) cassette. Upon removal of the stop codon, the actin promoter leads to constitutive expression of Gal4 and permanent induction of the

UAS transgenes. Using this method we titrated the heat-shocks to control the number of cells that express Gal4 and induced cells in the adult AG that overexpress Yki + E2F, Myc +E2F, or Tkv*. Overexpression of these growth regulators led to dramatic increases in nuclear size and DNA content, easily observable by Dapi staining in the adult accessory gland (Fig 5B). To confirm that the ectopic endocycles occur in the adult, we performed a one day EdU/sucrose feeding on animals at 10 days post eclosion with expression of Myc +E2F or Yki +E2F and observed extensive EdU incorporation in adult tissues (Fig 5C). The ease with which the main cells of the accessory gland can be induced to endocycle suggests that these cells may remain poised to enter the cell cycle in adults to maintain gland function.

Developmental control of variant cell cycles in the adult accessory gland

The FLP-FRT background we used to induce Myc, Tkv and Yki expression (Fig 5A) also contains a UAS-nuclear GFP (nlsGFP) to visualize which cells express Gal4. As described above, cells that are GFP positive and express Myc+E2F or Yki+E2F show enlarged nuclei (Fig 5B, Fig 6A). However, we noted that neighboring cells that appeared to be GFP negative also often exhibited an enlarged phenotype (Fig 6A). This led us to speculate that these cells may contain ring canals that allow neighboring cells to communicate in the adult AG.

Ring canals are created when cytokinesis is truncated and the cytokinetic furrow does not fully close and is instead stabilized. The resulting actin-rich structure creates an opening between cells through which cytoplasm is shared (McLean and Cooley 2014). Some, but not all cytoplasmic molecules can travel through these structures, and in particular nlsGFP travels through ring canals at a slow rate (McLean and Cooley 2014). We examined the localization of Pavarotti (Pav), a protein known to localize to ring canals in other Drosophila tissues. Using Pav tagged with GFP (Pav::GFP), we and others (Eikenes et al. 2013) observe localization consistent with the formation of ring canals in the adult AG (Fig 6C, top panel). We suggest that the non-autonomous growth effects we observe with Myc+E2F are due to Myc and/or E2F complexes passing through AG ring canals. Consistent with this idea, when we carefully quantify GFP fluorescence intensity, we find very low levels of GFP present in the immediate neighbor to the GFP positive cells (Fig 6B).

The location and number of ring canals in the adult AG displayed a distinct and reproducible pattern. Only one ring canal is present on each main cell and is located centrally on membranes at bicellular junctions. Two neighboring main cells can have a single ring canal between them, but no other ring canals between themselves and any other cells. This patterning suggests that ring canals are remnants of a truncated, penultimate cell cycle, generating sister cells prior to the binucleation event during AG development (Fig 6C, bottom panel). Importantly, Pav::GFP is not seen on the membrane of secondary cells, suggesting that these cells do not communicate via shared cytoplasm with their neighboring main cells. This supports a model for the developmentally regulated variant cell cycles of the *Drosophila* AG main cells that involves a progressive truncation of the canonical mitotic cell cycle. At 40-50 hrs APF we suggest a penultimate cell cycle occurs with a partially truncated cytokinesis to form ring canals in sister main cells. Around 50-60 hours APF, main cells undergo a further truncated cycle in which nuclear mitosis proceeds but cytokinesis does not occur at all, leading to bi-nucleation (Taniguchi et al. 2014). Then at 70-80h APF, the final cell cycle during metamorphosis is an endocycle completely lacking mitosis. The next endocycle begins within the first 5 hours of eclosion, prior to reproductive maturity to increase gland size. During adulthood the mature gland maintains the ability to endocycle to ensure gland function and size is maintained throughout the lifespan of the fly (Fig 6D).

Discussion

We find that under normal physiological conditions, cells of the adult AG endocycle and that this contributes to organ growth with age. Importantly, we show that this endocycling occurs both with and without mating and is maintained primarily in the main cell population. We used cell cycle reporters to verify hallmarks of the endocycle such as oscillations of the cell cycle degradation machinery. Additionally, we employed tissue damage protocols and expression of growth signals to trigger dramatic increases in endocycling. This work establishes that the adult accessory gland is not quiescent as previously suggested (Leiblich et al. 2012), but instead exhibits low levels of endocycling normally and remains poised to endocycle in response to specific signals in order to maintain accessory gland function.

Endocycling during gland maturation

We describe a wave of endocycling that occurs in most, if not all main cells of the AG, just after eclosion. This wave of endocycling and the resulting early gland growth is likely important for gland maturation and function. The identity of the signaling pathways that induce this early wave of endocycling is not known, but will be important for understanding AG maturation. Interestingly, a previous report found that secondary cell nuclei are smaller than main cell nuclei on the day of eclosion, prior to mating (Leiblich et al. 2012). This is consistent with our EdU and PCNA::GFP assays which show that this wave of endoreplication appears to be main cell-specific.

Endocycles in main vs. secondary cells

Under the conditions examined here, we find that secondary cell endocycles are very rare. This is supported by the patterns of oscillations we observe with cell cycle reporters, which suggest secondary cells are more refractory to endocycling than main cells. Our observations are in contrast to a recent preprint that shows secondary cells endocycle in a mating dependent manner and reports a lack of main cell endocycling (Leiblich et al. n.d.). There are a few possible reasons as to why we see such dramatic differences in levels and locations of AG endocycling. First, we used different genetic backgrounds in our studies. We examined the Canton-S strain as our wild-type control and used w^{1118} strains expressing a *paired-Gal4* transgene for our cell cycle reporter studies. Second, our mating protocols may differ. We performed mating under our normal crossing conditions (1:1.5 male to female ratio), rather than multiply-mated or mating-to-exhaustion protocols (Leiblich et al. 2012). Finally, there may be subtle differences in our culturing conditions that lead to differences in AG tissue homeostasis.

Our results using cell cycle reporter lines also hint at a possible mechanism for the differences we observe between main and secondary cell endocycles. We find that GFP-$E2F1_{1–230}$ appears stabilized in secondary cells, consistent with a lack of S-phase coupled degradation. By contrast, nls$Cdt1^{1-101}$-EBFP2 levels are dramatically lower in secondary cells than main cells. This is unexpected since in *Drosophila* the same CRL4(Cdt2) S-phase-dependent degradation is thought to be the major pathway for both CDT1 and E2F

destruction (Lee et al. 2010; Zielke et al. 2014). We suggest the nlsCdt1$^{1-101}$-EBFP2 may be degraded by another S-phase independent pathway in the secondary cells of the AG. Mammalian Cdt1 is also degraded via a Cdk2-regulated phosphodegron recognized by the SCF^{Skp2} pathway, but this pathway has been thought to play a minor role for *Drosophila* Cdt1 (Zielke et al. 2014). In flies the SCF^{Skp2} binding motif RRL contains a substitution to ARL, and the major Cdk2 phosphosite (T29/P in mammals) is not fully conserved. However, there is abundant evidence that fly Cdt1 is phosphorylated by CycE/Cdk2 on multiple sites (Thomer et al. 2004), including on a nearby site conserved in mammals (S31/P). Furthermore, an alternate potential SCF^{Skp2} binding RRL motif is found more N-terminally in fly Cdt1 (Supp. Fig 1), and some genetic evidence suggests fly Cdt1 can also be regulated by the SCF^{Skp2} complex in specific cell types (Kroeger et al., 2013). One of the two mammalian Cdk phosphosites in the more recently identified CDT1 PEST domain sequence are conserved in flies and present in the CDT1-BFP construct, but was not interrogated in a previous study of phosphomutant Cdt1 (Thomer et al. 2004; Handke et al). We therefore suggest the CDT1-BFP construct could reflect more elaborate Cdt1 regulation than just CRL4(Cdt2) S-phase degradation. Altogether our data suggests secondary cells exhibit rare endocycles under normal physiological conditions, possibly due to specific regulation of replication licensing through secondary-cell specific Cdt1 degradation. This may allow secondary cells to remain poised for endocycle entry upon specific signals.

Control of AG endocycling

We show that main cells of the AG remain poised to endocycle and upregulation of positive regulators of cell growth and proliferation, implicated in damage response mechanisms, are sufficient to induce endocycling. We suggest this underlies the ability of the AG to recover from damage and return to a more normal size (Fig. 3D). However, one key aspect of compensatory growth and tissue regeneration we have not addressed is restoration of gland function. We are currently investigating how damage alters gland function and whether the recovery protocol we use also allows the gland to regain function.

Our data has revealed additional variant cell cycles during AG development. We show evidence that a penultimate cell cycle with a truncated cytokinesis occurs in the developing gland during metamorphosis to form ring canals and we find a very early wave

of endocycling that occurs in the adult AG within hours of eclosion, independent of feeding or exposure to females. Our results reveal a more complete picture of cell cycle regulation in the AG, where the cell cycle is progressively truncated during the later stages of metamorphosis resulting in a binucleate and polyploid tissue (Fig. 6D). Polyploidy further increases during adulthood through additional endocycles under normal tissue homeostasis. This demonstrates the AG is an excellent model system for studying multiple types of variant cell cycles in a developmental context.

Materials and Methods

Fly stocks:
Canton S
Fly FUCCI (BL55122) w[1118]; Kr[If-1]/CyO, P{ry[+t7.2]=en1}wg[en11]; P{w[+mC]=UAS-GFP.E2f1.1-230}26 P{w[+mC]=UAS-mRFP1.NLS.CycB.1-266}17/TM6B, Tb
RGB Cell Cycle Sensor - P{w{+mC}=UAS-nlsCdt1N101EBFP2-T2A-nlsCycBN96-nlsCycBN285tdTomato-T2A-EGFPPCNA} II.1 (UAS-RGB cell cycle tracker).
Prd-Gal4 (BL1947) w[*]; Prd-Gal4/TM3, Sb[1]
EGFP::PCNA (provided by S. Blythe)
DEMISE lines : all data shown is with line 10-3; pUAST-FRT-Stop-FRT-rpr/CyO – (provided by D. Fox Lab)
y,w,hs-flp; ; Prd-gal 4/TM6B (y,w,hs-flp^{12} and BL1947)
w; UAS-P35/Cyo-GFP; act>CD2>gal4,UAS-GFP(nls)/TM3-Ser-GFP
y,w,hs-flp; + ; +
y,w,hs-flp; UAS-E2F, UAS-DP/Cyo-GFP; UAS-dMyc^{42}/TM6B (UAS E2F1,UAS DP from Neufeld et al 1998, dMyc from BL#9675)
y,w,hs-flp; UAS-E2F1, UAS-Dp/CyO-GFP; UAS-Yki^{s111,168,250}/TM6B (UAS E2F1,UAS DP from Neufeld et al 1998, Yki^{s111,168,250} from BL#28817)
y,w,hs-flp; UAS-Tkv* (UAS Tkv* is UAS-Tkv^{Q235D} from (Nellen et al., 1996)
Pav::GFP (provided by Y. Yamashita) Ubiquitin-PAV::GFP; nanos-gal4

Fly rearing and mating:
All flies were raised and kept at room temperature (23°C) on Bloomington Cornmeal food unless otherwise noted. For experiments with virgins: males were collected as virgins and aged for indicated times in vials containing 7-10 males. For experiments with mated animals: males and females were kept at an approximate 1:1.5 ratio for indicated times.

Tissue fixation and staining:
Accessory glands were dissected in 1X PBS and were fixed in 4% PFA+1xPBS for 30 min at room temperature while rocking. Tissues were rinsed with 1xPBS+0.1%Triton-X twice for 10 minutes. Tissues were further permeabilized in 1xPBS+1.0%Triton-X for 30 minutes at room temperature while rocking. Tissues were rinsed with PAT for 10 min and primary antibodies diluted in fresh PAT were incubated at room temperature rocking overnight. Tissues were rinsed twice for 10 minutes in 1xPBS+0.1%Triton-X. Tissues were pre-blocked in PBT-X+2%NGS for 10 minutes. Secondary antibody was added to fresh PBT-X+2%NGS and tissues were incubated overnight

rotating at room temperature. Tissues were rinsed twice in 1xPBS+0.1%Triton-X before incubating in DAPI (1µg/ml) for 10 min. Tissues were rinsed thoroughly before mounting with Vectashield.

The following antibodies were used in this study: Mouse anti DLG (DHSB) 1:500, Rabbit anti PH3 (Millipore #06-570) 1:1000, mouse anti PH3 (Cell Signaling #9706) 1:1000.

Measurements:
Fluorescent images were obtained using a Leica SP5 confocal, Leica SP8 confocal or Leica DMI6000B epifluorescence system. Brightfield images used to quantify gland size were taken on a Leitz Orthoplan.

To obtain overall gland size measurements, images were imported to Adobe Photoshop and Lasso Tool was used to outline the lobe of the accessory gland. Photoshop Measure was used to quantify pixels within the gland and measurements were transferred to Prism for analysis.

Discs large (DLG) antibody staining was used for all cell size measurements. Due to the apical localization of DLG, cell size measurements reported here are not of the volume of a cell, but rather a measurement of the apical area. Measurements reported here are taken mid-lobe and are only of main cells to ensure cell type differences are not confounding our measurements. Image J was used to obtain measurements of cells in microns and measurements were transferred to Prism for analysis.

Nuclear area measurements were done similarly to Cell Size (described above) using DAPI signal and are of main cells only.

To measure levels of GFP, Cdt1-BFP and GFP-E2F1, Image J was used to measure integrated density of fluorescence within nuclei of secondary and main cells. Corrected total cell fluorescence (CTCF) was calculated following CTCF = Integrated Density – (Area of selected nuclei*mean fluorescence of background). https://theolb.readthedocs.io/en/latest/imaging/measuring-cell-fluorescence-using-imagej.html

EdU labeling:
Click-IT EdU AlexaFluor-555/488 Imaging kits were used as directed (Life Technologies).
For labeling on the day of eclosion, accessory glands were dissected and immediately placed into Ringers solution containing 1mM EdU for 1 hour prior to fixing.
For labeling during adult lifespan, animals were fed 1 mM EdU in 10% sucrose with blue food coloring for the indicated amounts of time. EdU/sucrose mixture was placed on whatman paper within empty vials and was changed every 2-3 days to control for contamination. We also performed feeding with 1 mM EdU in Cornmeal food with blue food coloring for up to 6 days and obtained similar results.

DEMISE:
Genotype used to induce damage was y,w,hs-flp; DEMISE 10-3/+; Prd-Gal4/+.
When kept at room temperature, on the day of eclosion animals already show DEMISE induced damage. For recovery experiments animals were collected as virgins and shifted to 18°C to reduce the Gal4/UAS expression levels. For EdU experiments animals were fed EdU/sucrose as described above for the indicated amounts of time.

Induction of growth regulators
Genotypes used:

y,w,hsflp; UAS-E2F1, UAS-DP/UAS-p35; act>CD2>gal4,UAS-GFP(nls)/ UAS-dMyc
y,w,hsflp; UAS-E2F1, UAS-DP/ UAS-p35; act>CD2>gal4,UAS-GFP(nls)/ UAS-Yki ^{s111,168,250}
y,w,hsflp; +; act>CD2>gal4,UAS-GFP(nls)/ UAS-Tkv*
For EdU labeling: Newly eclosed flies were heat-shocked at 37°C for 60sec and aged for five days. Flies were fed EdU/sucrose as described above for 24 hours prior to dissection.

Acknowledgements:

We thank members of the Buttitta and Taichman Labs for advice and discussions, especially Ajai Pulianmackal, Dr. Frank Cackowski and Dr. Kenji Yumoto. We thank Pusparanee Hakim and Ce Wang for help with early experiments characterizing the fly AG. We thank the following for kindly providing fly lines: Shelby Blythe for PCNA::GFP, Yukiko Yamashita for Pav::GFP, Erez Cohen and Don Fox for DEMISE lines, and Christian Lehner for the RGB line. This work was supported by a Prostate Cancer Foundation Challenge Award (16CHAL05). A. Box was supported by the University of Michigan Organogenesis Predoctoral Training Grant (NIH T32 HD007505). S.J. Church was supported by a University of Michigan Rackham Merit Fellowship and S. Nandakumar was supported by a University of Michigan Barbour Scholar Award.

Adams, Erika M., and Mariana F. Wolfner. 2007. "Seminal Proteins but Not Sperm Induce Morphological Changes in the Drosophila Melanogaster Female Reproductive Tract during Sperm Storage." *Journal of Insect Physiology* 53 (4): 319–31. https://doi.org/10.1016/j.jinsphys.2006.12.003.

Ahmad, Shaad M., and Bruce S. Baker. 2002. "Sex-Specific Deployment of FGF Signaling in Drosophila Recruits Mesodermal Cells into the Male Genital Imaginal Disc." *Cell* 109: 651–61.

Bairati, Aurelio. 1968. "STRUCTURE AND ULTRASTRUCTURE OF THE MALE REPRODUCTIVE SYSTEM IN DROSOPHILA MELANOGASTER MEIG." *Italian Journal of Zoology*, 105–82.

Bertram, Michael J., Geetanjali A. Akerkar, Robert L. Ard, Cayetano Gonzalez, and Mariana F. Wolfner. 1992. "Cell Type-Specific Gene Expression in the Drosophila Melanogaster Male Accessory Gland." *Mechanisms of Development* 38 (1): 33–40. https://doi.org/10.1016/0925-4773(92)90036-J.

Blythe, Shelby A, and Eric F Wieschaus. 2016. "Establishment and Maintenance of Heritable Chromatin Structure during EarlyDrosophilaembryogenesis." *ELife* 5. https://doi.org/10.7554/eLife.20148.

Cohen, Erez, Scott R Allen, Jessica K Sawyer, and Donald T Fox. 2018. "Fizzy-Related Dictates A Cell Cycle Switch during Organ Repair and Tissue Growth Responses in the Drosophila Hindgut." *ELife* 7 (August). https://doi.org/10.7554/eLife.38327.

Edgar, Bruce A., Norman Zielke, and Crisanto Gutierrez. 2014. "Endocycles: A Recurrent Evolutionary Innovation for Post-Mitotic Cell Growth." *Nature Reviews Molecular Cell Biology* 15 (3): 197–210. https://doi.org/10.1038/nrm3756.

Eikenes, Åsmund H, Andreas Brech, Harald Stenmark, and Kaisa Haglund. 2013. "Spatiotemporal Control of Cindr at Ring Canals during Incomplete Cytokinesis in the Drosophila Male Germline." *Developmental Biology* 377 (1): 9–20. https://doi.org/10.1016/j.ydbio.2013.02.021.

Grendler, Janelle, Sara Lowgren, Monique Mills, and Vicki P. Losick. 2019. "Wound-Induced Polyploidization Is Driven by Myc and Supports Tissue Repair in the Presence of DNA Damage." *Development*, July 17, pii: dev.173005. doi: 10.1242/dev.173005. [Epub

ahead of print]

Handke, Björn, János Szabad, Peter V. Lidsky, Ernst Hafen, and Christian F. Lehner. 2014. "Towards Long Term Cultivation of Drosophila Wing Imaginal Discs In Vitro." *PLoS ONE* 9 (9): e107333. https://doi.org/10.1371/journal.pone.0107333.

Heifetz, Y., L. N. Vandenberg, H. I. Cohn, and M. F. Wolfner. 2005. "Two Cleavage Products of the Drosophila Accessory Gland Protein Ovulin Can Independently Induce Ovulation." *Proceedings of the National Academy of Sciences* 102 (3): 743–48. https://doi.org/10.1073/pnas.0407692102.

Inge Øvrebø, Jan, and Bruce A Edgar. 2018. "Polyploidy in Tissue Homeostasis and Regeneration." *Development* vol. 145 https://doi.org/10.1242/dev.156034.

Koppik, Mareike, Jan-Hendrik Specker, Ina Lindenbaum, and Claudia Fricke. 2018. "Physiological Maturation Lags Behind Behavioral Maturation in Newly Eclosed Drosophila Melanogaster Males." *The Yale Journal of Biology and Medicine* 91 (4): 399–408. http://www.ncbi.nlm.nih.gov/pubmed/30588207.

Kroeger PT Jr1, Shoue DA, Mezzacappa FM, Gerlach GF, Wingert RA, Schulz RA. 2013. "Knockdown of SCF(Skp2) function causes double-parked accumulation in the nucleus and DNA re-replication in Drosophila plasmatocytes." *PLoS One*. Oct 24;8(10):e79019. doi: 10.1371/journal.pone.0079019.

Lee, Hyun O., Sima J. Zacharek, Yue Xiong, and Robert J. Duronio. 2010. "Cell Type–Dependent Requirement for PIP Box–Regulated Cdt1 Destruction During S Phase." Edited by Orna Cohen-Fix. *Molecular Biology of the Cell* 21 (21): 3639–53. https://doi.org/10.1091/mbc.e10-02-0130.

Leiblich, Aaron, Josephine E E U Hellberg, Aashika Sekar, Carina Gandy, Mark Wainwright, Pauline Marie, Deborah C I Goberdhan, Freddie C Hamdy, and Clive Wilson. n.d. "Mating Induces Switch From Hormone-Dependent to –Independent Steroid Receptor-Mediated Growth in Drosophila Prostate-Like Cells." *BioRxiv* Jan 29, 2019. https://doi.org/10.1101/533976.

Leiblich, Aaron, Luke Marsden, Carina Gandy, Laura Corrigan, Rachel Jenkins, Freddie Hamdy, and Clive Wilson. 2012. "Bone Morphogenetic Protein- and Mating-Dependent Secretory Cell Growth and Migration in the Drosophila Accessory Gland." *Proceedings of the National Academy of Sciences of the United States of America* 109 (47): 19292–97.

https://doi.org/10.1073/pnas.1214517109.

Losick, Vicki P., Donald T. Fox, and Allan C. Spradling. 2013. "Polyploidization and Cell Fusion Contribute to Wound Healing in the Adult Drosophila Epithelium." *Current Biology* 23 (22): 2224–32. https://doi.org/10.1016/J.CUB.2013.09.029.

Losick, Vicki P., Albert S. Jun, and Allan C. Spradling. 2016. "Wound-Induced Polyploidization: Regulation by Hippo and JNK Signaling and Conservation in Mammals." *PLOS ONE* 11 (3): e0151251. https://doi.org/10.1371/journal.pone.0151251.

Lung, O., L. Kuo, and M.F. Wolfner. 2001. "Drosophila Males Transfer Antibacterial Proteins from Their Accessory Gland and Ejaculatory Duct to Their Mates." *Journal of Insect Physiology* 47 (6): 617–22. https://doi.org/10.1016/S0022-1910(00)00151-7.

McLean, Peter F, and Lynn Cooley. 2014. "Bridging the Divide: Illuminating the Path of Intercellular Exchange through Ring Canals." *Fly* 8 (1): 13–18. https://doi.org/10.4161/fly.27016.

Narbonne-Reveau, Karine, Stefania Senger, Margit Pal, Anabel Herr, Helena E Richardson, Maki Asano, Peter Deak, and Mary A Lilly. 2008. "APC/CFzr/Cdh1 Promotes Cell Cycle Progression during the Drosophila Endocycle." *Development (Cambridge, England)* 135 (8): 1451–61. https://doi.org/10.1242/dev.016295.

Nellen D, Burke R, Struhl G, Basler K. 1996. Direct and long‐range action of a DPP morphogen gradient. *Cell* 85: 357‐368.

Neufeld TP, de la Cruz AF, Johnston LA, Edgar BA. 1998. Coordination of growth and cell division in the Drosophila wing. *Cell* 93: 1183– 1193.

Orr-Weaver, Terry L. 2015. "When Bigger Is Better: The Role of Polyploidy in Organogenesis HHS Public Access." *Trends Genet* 31 (6): 307–15. https://doi.org/10.1016/j.tig.2015.03.011.

Pozo, Pedro N, and Jeanette Gowen Cook. 2016. "Regulation and Function of Cdt1; A Key Factor in Cell Proliferation and Genome Stability." *Genes* 8 (1): 2. https://doi.org/10.3390/genes8010002.

Prince, Elodie, Benjamin Kroeger, Dragan Gligorov, Clive Wilson, Suzanne Eaton, François Karch, Marko Brankatschk, and Robert K. Maeda. 2019. "Rab-Mediated Trafficking in

the Secondary Cells of *Drosophila* Male Accessory Glands and Its Role in Fecundity." *Traffic* 20 (2): 137–51. https://doi.org/10.1111/tra.12622.

Qazi, Margaret C. Bloch, and Mariana F. Wolfner. 2003. "An Early Role for the Drosophila Melanogaster Male Seminal Acp36DE in Female Sperm Storage." *Journal of Experimental Biology* 206 (19): 3521–28. https://doi.org/10.1242/JEB.00585.

Ravi Ram, K., S. Ji, and M.F. Wolfner. 2005. "Fates and Targets of Male Accessory Gland Proteins in Mated Female Drosophila Melanogaster." *Insect Biochemistry and Molecular Biology* 35 (9): 1059–71. https://doi.org/10.1016/J.IBMB.2005.05.001.

Sitnik, J. L., D. Gligorov, R. K. Maeda, F. Karch, and M. F. Wolfner. 2016. "The Female Post-Mating Response Requires Genes Expressed in the Secondary Cells of the Male Accessory Gland in Drosophila Melanogaster." *Genetics* 202 (3): 1029–41. https://doi.org/10.1534/genetics.115.181644.

Stetina, Jessica R Von, Laura E Frawley, Yingdee Unhavaithaya, and Terry L Orr-Weaver. 2018. "Variant Cell Cycles Regulated by Notch Signaling Control Cell Size and Ensure a Functional Blood-Brain Barrier." *Development (Cambridge, England)* 145 (3). https://doi.org/10.1242/dev.157115.

Susic-Jung, Loreen, Christina Hornbruch-Freitag, Jessica Kuckwa, Karl-Heinz Rexer, Uwe Lammel, and Renate Renkawitz-Pohl. 2012. "Multinucleated Smooth Muscles and Mononucleated as Well as Multinucleated Striated Muscles Develop during Establishment of the Male Reproductive Organs of Drosophila Melanogaster." *Developmental Biology* 370 (1): 86–97. https://doi.org/10.1016/J.YDBIO.2012.07.022.

Tamori, Yoichiro, and Wu-Min Deng. 2013a. "Compensatory Cellular Hypertrophy: The Other Strategy for Tissue Homeostasis." https://doi.org/10.1016/j.tcb.2013.10.005.

———. 2013b. "Tissue Repair through Cell Competition and Compensatory Cellular Hypertrophy in Postmitotic Epithelia." *Developmental Cell* 25 (4): 350–63. https://doi.org/10.1016/j.devcel.2013.04.013.

Taniguchi, Kiichiro, Akihiko Kokuryo, Takao Imano, Ryunosuke Minami, Hideki Nakagoshi, and Takashi Adachi-Yamada. 2014. "Isoform-Specific Functions of Mud/NuMA Mediate Binucleation of Drosophila Male Accessory Gland Cells." *BMC Developmental Biology* 14 (December): 46. https://doi.org/10.1186/s12861-014-0046-5.

Thomer, M., Noah R May, Bhagwan D Aggarwal, Garrick Kwok, and Brian R Calvi. 2004.

"Drosophila Double-Parked Is Sufficient to Induce Re-Replication during Development and Is Regulated by Cyclin E/CDK2." *Development* 131 (19): 4807–18. https://doi.org/10.1242/dev.01348.

Wilson, C., A. Leiblich, D.C.I. Goberdhan, and F. Hamdy. 2017. "The Drosophila Accessory Gland as a Model for Prostate Cancer and Other Pathologies." In *Current Topics in Developmental Biology*, 121:339–75. https://doi.org/10.1016/bs.ctdb.2016.06.001.

Zhou, Jun, Sebastian Florescu, Anna-Lisa Boettcher, Lichao Luo, Devanjali Dutta, Grainne Kerr, Yu Cai, Bruce A. Edgar, and Michael Boutros. 2015. "Dpp/Gbb Signaling Is Required for Normal Intestinal Regeneration during Infection." *Developmental Biology* 399 (2): 189–203. https://doi.org/10.1016/J.YDBIO.2014.12.017.

Zielke, N., S. Querings, C. Rottig, C. Lehner, and F. Sprenger. 2008. "The Anaphase-Promoting Complex/Cyclosome (APC/C) Is Required for Rereplication Control in Endoreplication Cycles." *Genes & Development* 22 (12): 1690–1703. https://doi.org/10.1101/gad.469108.

Zielke, Norman, Kerry J. Kim, Vuong Tran, Shusaku T. Shibutani, Maria-Jose Bravo, Sabarish Nagarajan, Monique van Straaten, et al. 2011. "Control of Drosophila Endocycles by E2F and CRL4CDT2." *Nature* 480 (7375): 123–27. https://doi.org/10.1038/nature10579.

Zielke, Norman, Jerome Korzelius, Monique van Straaten, Katharina Bender, Gregor F.P. Schuhknecht, Devanjali Dutta, Jinyi Xiang, and Bruce A. Edgar. 2014. "Fly-FUCCI: A Versatile Tool for Studying Cell Proliferation in Complex Tissues." *Cell Reports* 7 (2): 588–98. https://doi.org/10.1016/J.CELREP.2014.03.020.

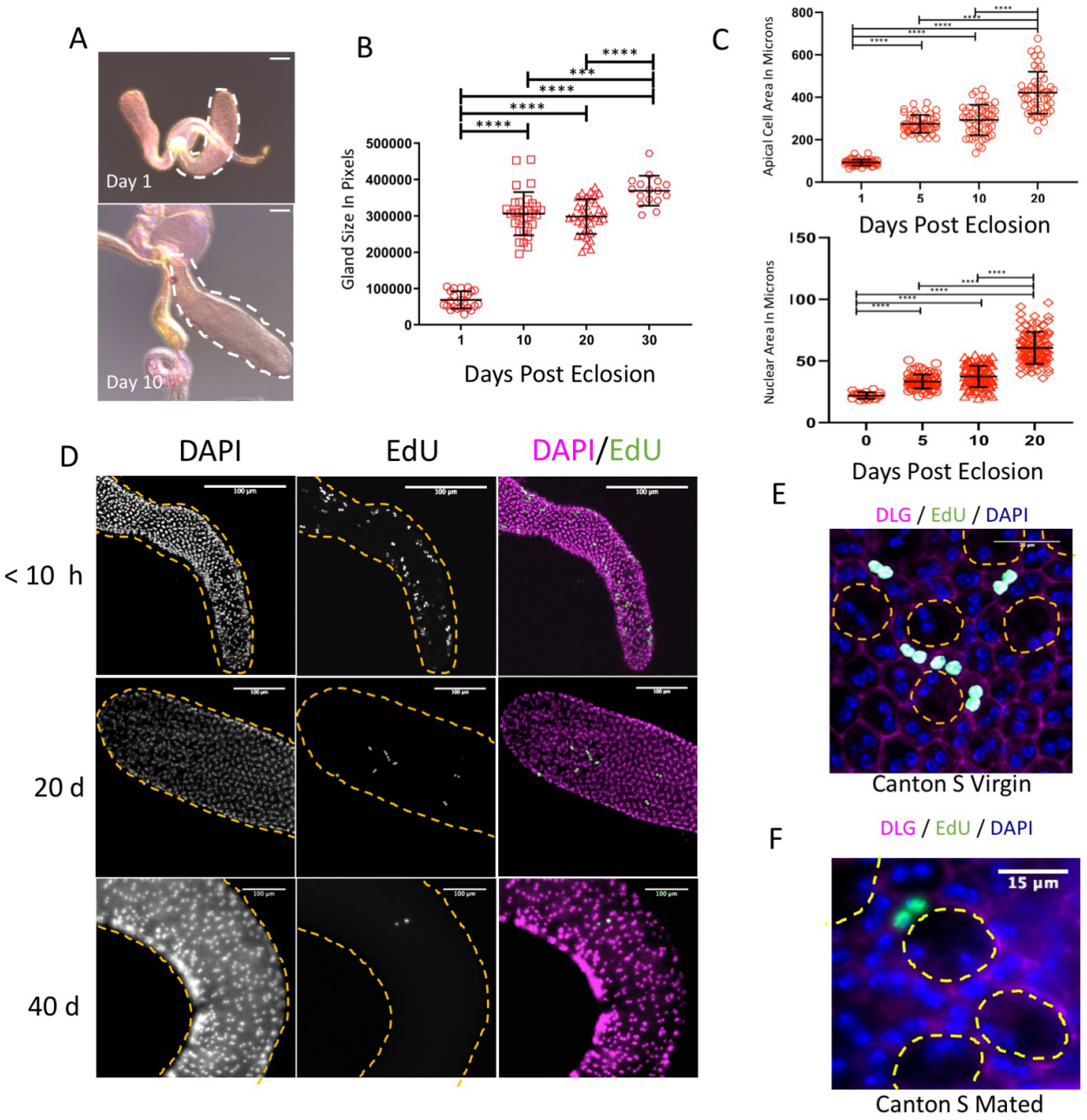

Figure 1: The adult accessory gland grows and main cells endoreplicate under normal physiological conditions throughout lifespan.

A: Adult accessory glands at Day 1 (day of eclosion) and Day 10 post eclosion. Accessory gland lobe is outlined with white dashed line. All glands measured are from virgins, so that size effects due to mating (i.e. release of seminal fluid proteins, hormonal signaling, muscle contractions, and emptying of the lumen) would not confound the measurements obtained. B: Quantification of adult virgin male accessory gland area in pixels at indicated ages.

C: Quantification of adult virgin male accessory gland cell size and nuclear size in microns at indicated ages.
D: EdU incorporation assays in virgin male accessory glands. Accessory glands are outlined with yellow dashed line.
E: Magnification of virgin male accessory gland from 10 day EdU feeding at 20 day timepoint. EdU+ cells are main cells located near the distal tip of the gland. Secondary cells are outlined with yell0w dashed line.
F: Magnification of mated male accessory gland. EdU+ cell is a main cell near the distal tip of the gland. Secondary cells are outlined with yellow.
Statistics are one-way ANOVA:
**** $p < 0.0001$
*** $p = 0.0002$
Scale bars:
A,D: 100 microns, E: 25 microns, F: 15 microns

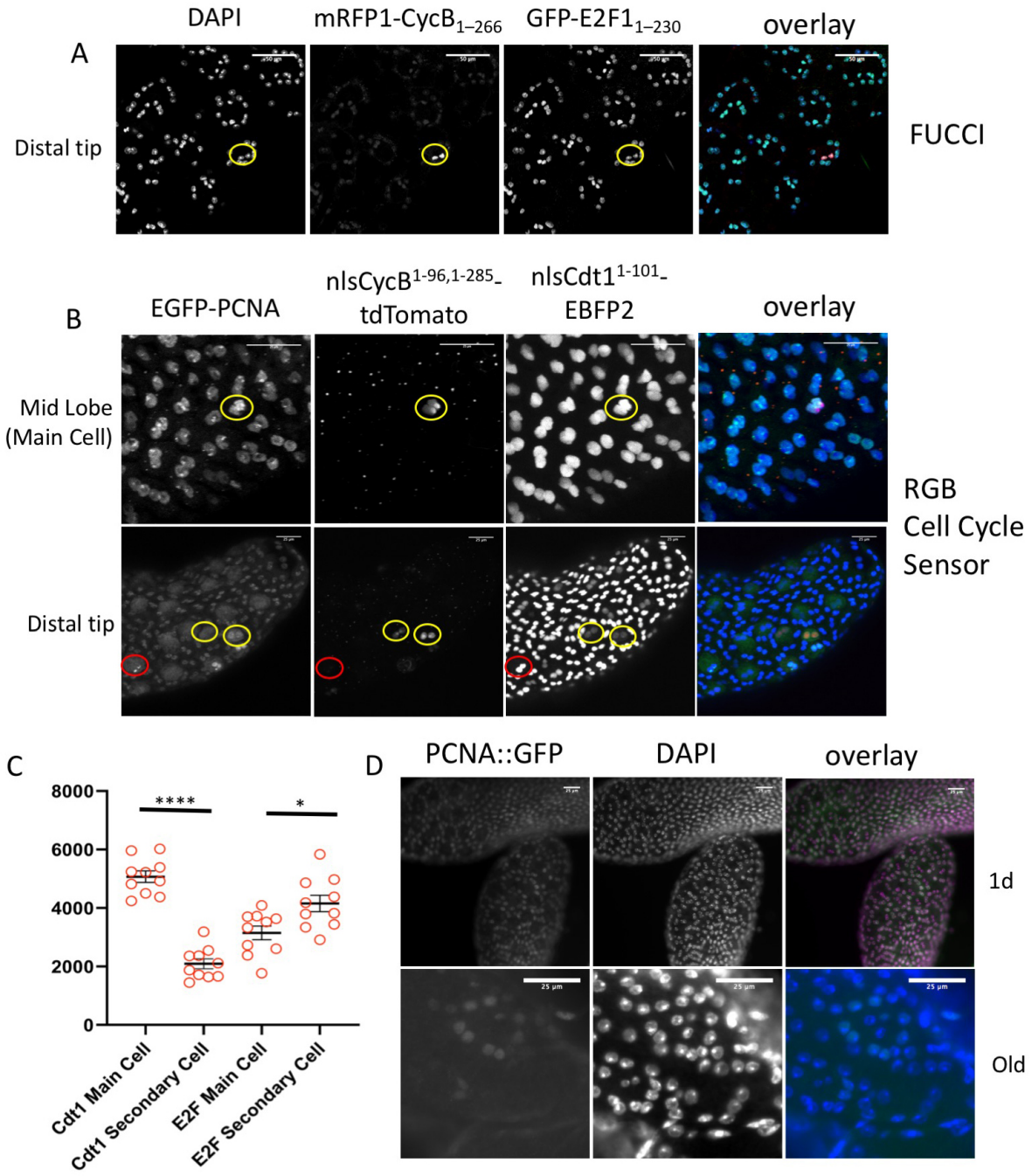

Figure 2: Cell cycle degradation machinery oscillates in the adult accessory gland.

A: Fly FUCCI in the adult accessory gland. Cell cycle protein degrons mRFP1-CycB$_{1–266}$, to assay APC/C activity, and GFP-E2F1$_{1–230}$, to assay CRL4 (Cdt2) activity. The tissue has high APC/C activity, except in a small subset of cells, outlined in yellow.

B: RGB cell cycle sensor in the adult accessory gland. Full length EGFP-PCNA to visualize early S Phase and cell cycle protein degrons nlsCycB$^{1-96}$-nlsCycB$^{1-285}$-tdTomato, to assay APC/C activity, and nlsCdt1$^{1-101}$-EBFP2, to assay CRL4 (Cdt2) activity. APC/C activity is high

throughout the tissue, except in a small subset of cells, outlined in yellow. Few cells exhibit PCNA foci, indicating early S Phase, outlined in red.
(Top panel) Mid lobe-region showing oscillations in main cells and (lower panel) distal tip showing oscillations in secondary cells.

C: Quantification of fluorescence intensity of GFP-E2F1$_{1-230}$ and nlsCdt1$^{1-101}$-EBFP2, from (A) and (B).

D: Endogenous PCNA tagged with GFP in the adult accessory gland.
Statistics are ANOVA:
**** $p < 0.0001$
* p =
Scale bars:
A: 50 microns
B,D : 25 microns

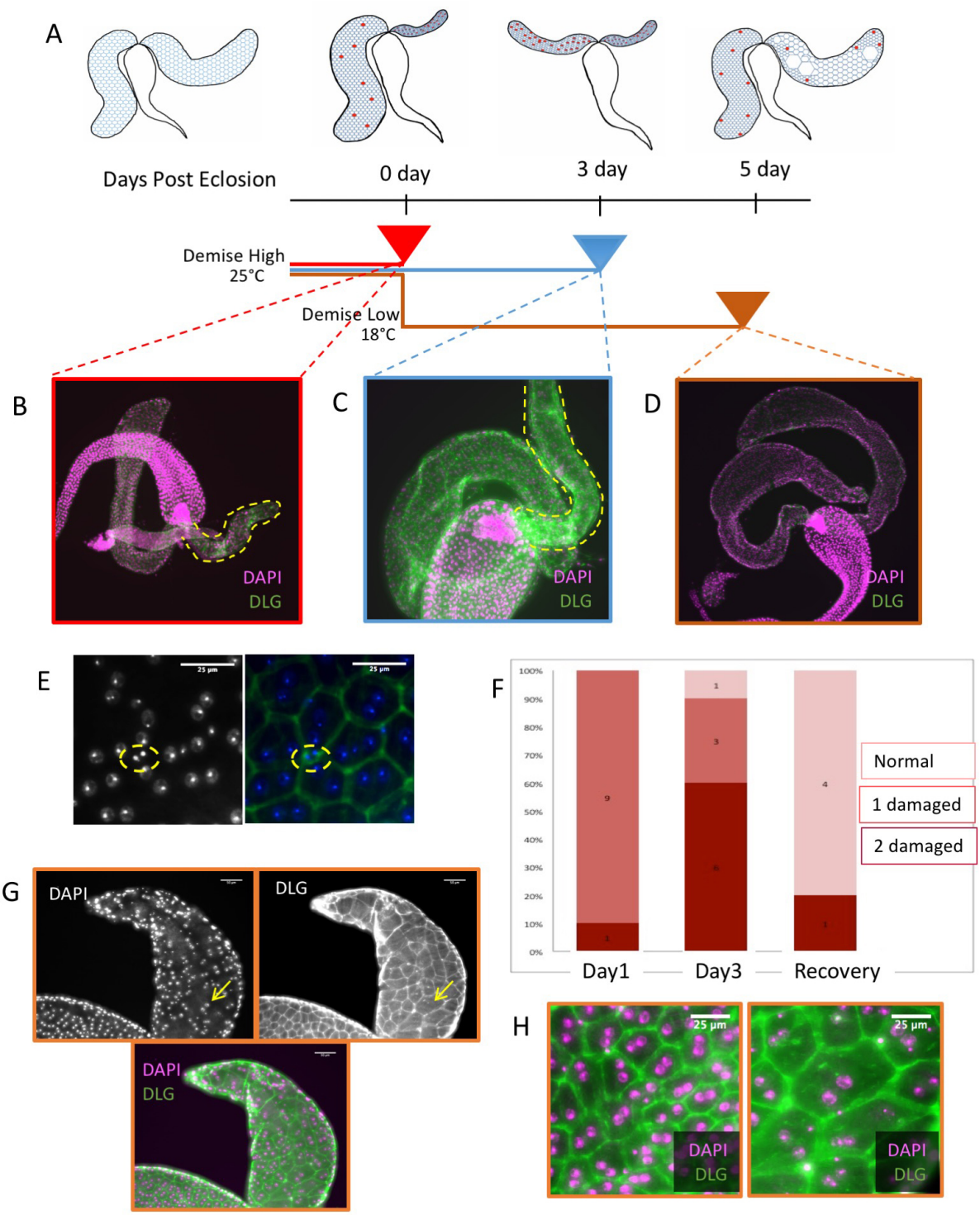

Figure 3: The adult accessory gland exhibits compensatory cellular hypertrophy in response to damage.

A: Schematic of experimental procedure and representative outcomes using DEMISE system and a recovery protocol in the accessory gland. Red cells are representative of cells in which DEMISE is active and Reaper expression is high.

B: DEMISE system in the adult accessory gland at day of eclosion. Damaged lobe is outlined in yellow

C: DEMISE system in the adult accessory gland at day 3 at room temperature. Damaged lobe is outlined in yellow

D: DEMISE system in adult accessory gland that has been shifted to 18°C for 5 day recovery protocol.

E: DEMISE induced damage is visualized as pyknotic nuclei. Outlined with yellow dashed line is a binucleate accessory gland cell with two pyknotic nuclei.

F: Quantification of DEMISE system induced damage and accessory gland phenotype via categories of: normal size lobes, 1 damaged lobe, or 2 damaged lobes.

G: DEMISE induced damage with recovery protocol has one normal lobe that has undergone very low levels of damage and one lobe that has undergone damage and responded with compensatory cellular hypertrophy (yellow arrow).

H: Magnification of both DEMISE accessory gland lobes from recovery protocol (D). One lobe with normal cell size (left) and one lobe that has undergone compensatory cellular hypertrophy (right).

Scale bars:
E,H: 25 microns, G: 50 microns

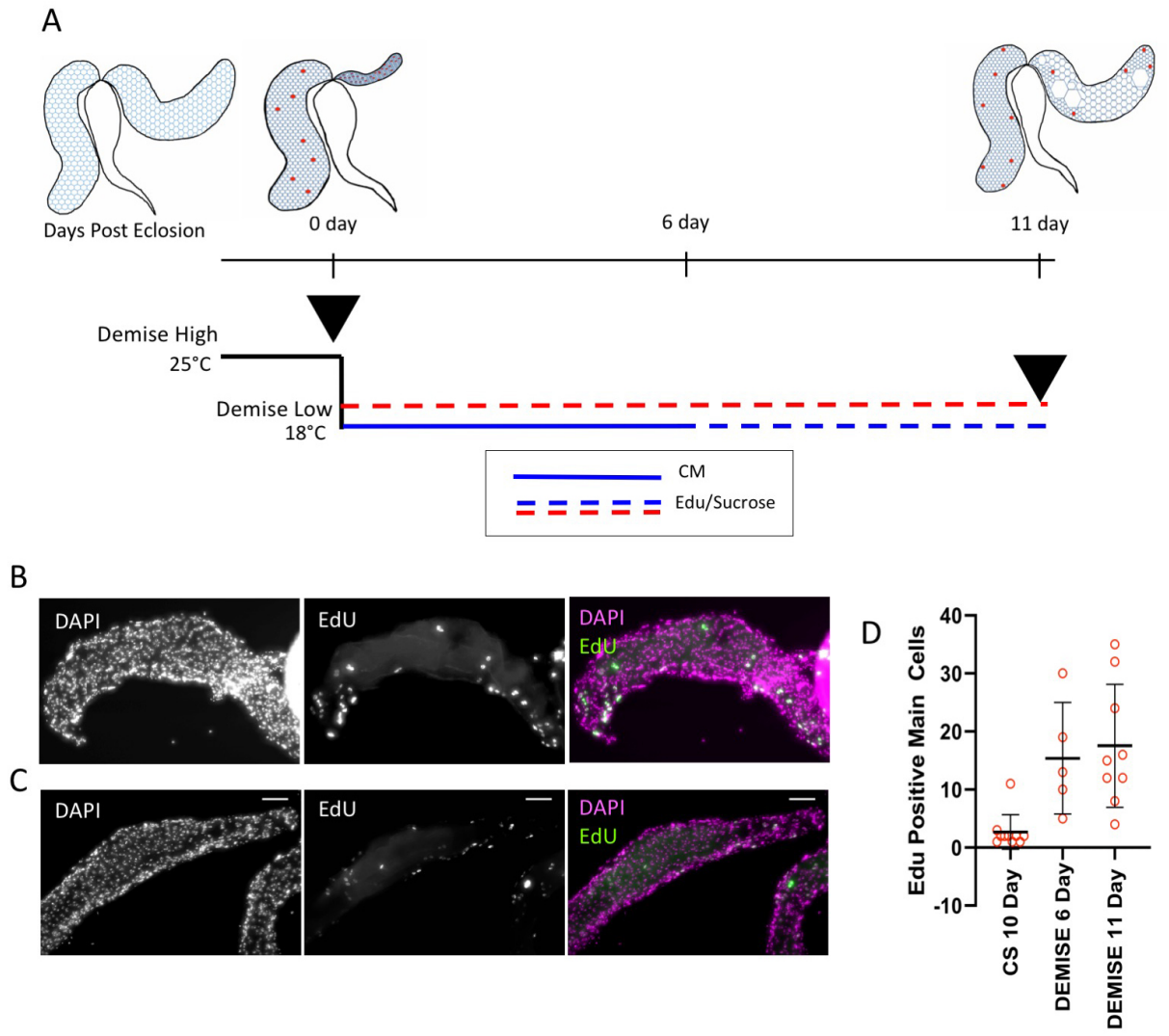

Figure 4: The adult accessory gland increases endoreplication in response to tissue damage.

A: Schematic of experimental procedure and representative outcomes using DEMISE system to induce damage and recovery protocol in the accessory gland paired with EdU feeding for different lengths of time.

B: DEMISE accessory gland from male that was fed EdU for the entire 11 day recovery protocol.

C: DEMISE accessory gland from male that was fed EdU for only the last 5 days of the 11 day recovery protocol.

D: Quantification of EdU+ main cells for a 7 day RT feeding and EdU feeding for the entire 11 day recovery protocol (approx. 5 days RT).

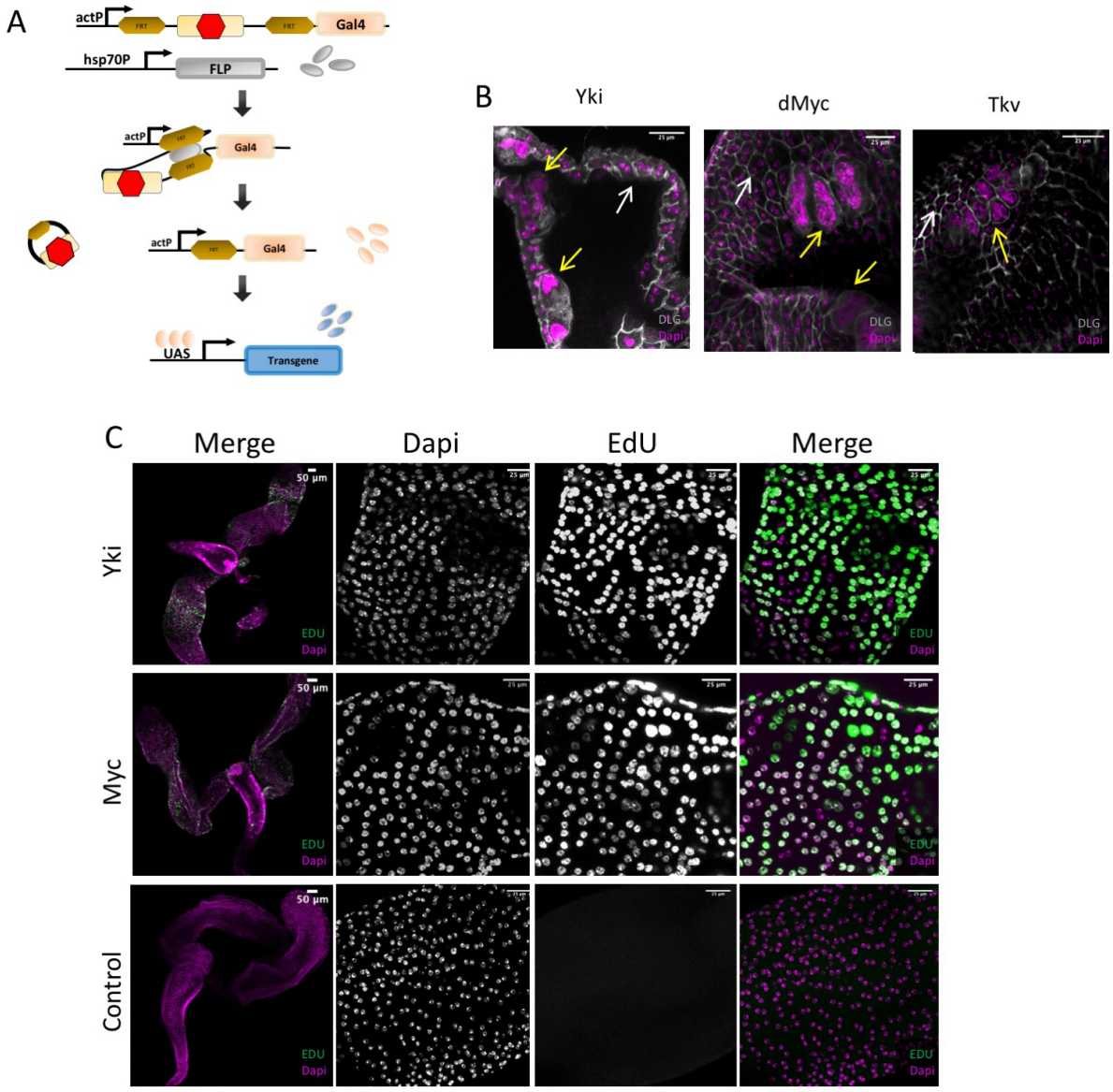

Figure 5: Cells of the adult accessory gland are poised to endocycle.

A) The Flippase-FRT system used to activate gene expression in clones in the adult accessory gland.

B) Overexpression of factors that promote cell cycle entry lead to increased nuclear size in the adult accessory gland. White arrows: normal nuclear morphology, Yellow arrows: enlarged nuclei.

C) EdU incorporation in the adult accessory gland upon overexpression of the indicated growth regulators.

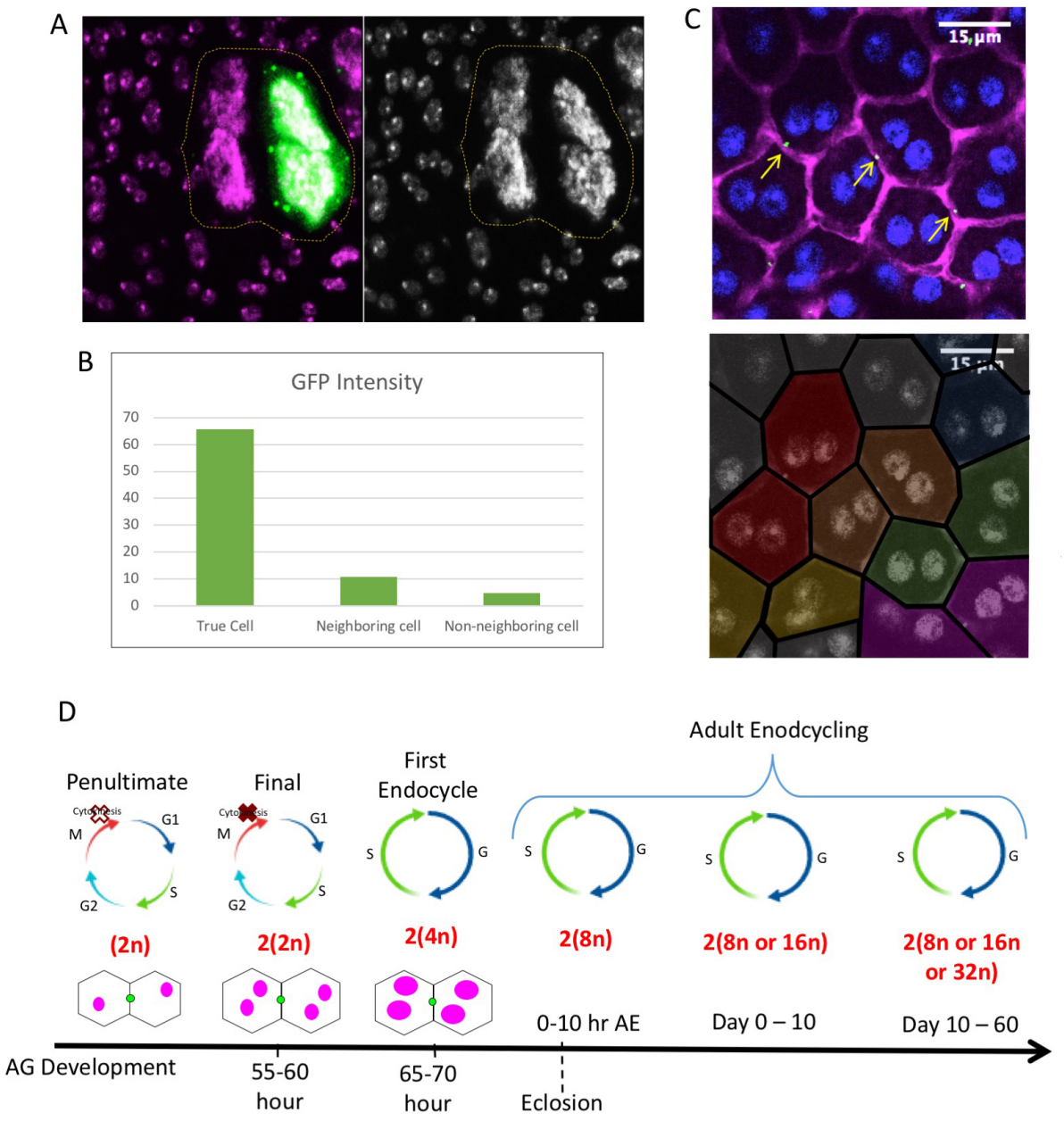

Figure 6: Developmental control of the cell cycle in the Drosophila accessory gland.

A: GFP negative cells show enlarged nuclei upon clone induction; these cells neighbor GFP-high cells.

B: Quantification of GFP levels from Fig 6A. Quantifications were taken of GFP-high cell, the GFP-low neighbor with the enlarged nuclei, and non-neighboring GFP negative cells (to subtract background). GFP in cells neighboring specific GFP-high cells is only visible when overexposing the GFP signal.

C: Pavarotti::GFP in the accessory gland. The localization of Pav::GFP (yellow arrow) suggests that main cells are in sister pairs from the penultimate cell cycle when the ring canal is formed. (Sister-pairs are shown here in a psuedocolored overlay.)

D: A model for variant cell cycle regulation in the developing accessory gland main cells. Progressive truncations of cytokinesis and mitosis culminate in endocycling that persists into adult stages.

Supplemental Figure

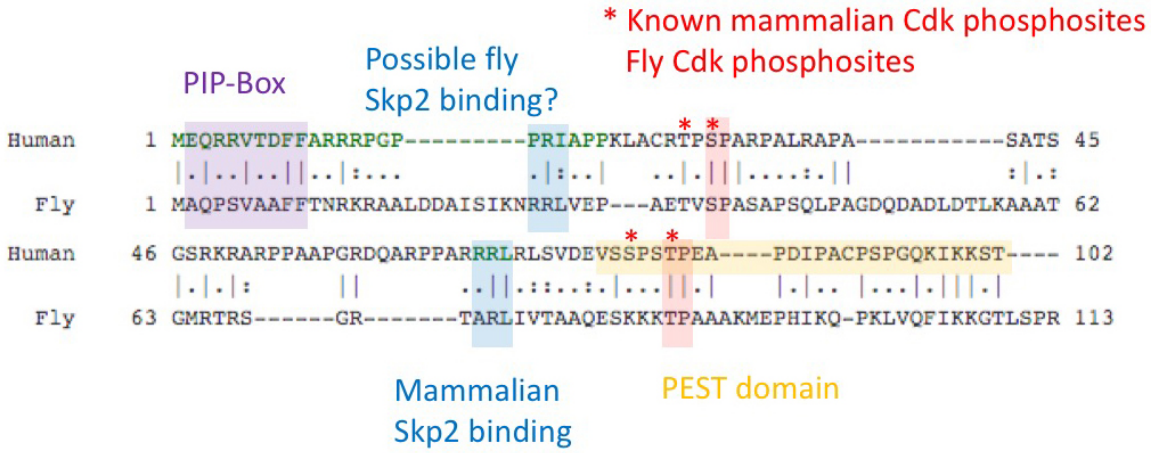

Supp. Fig. 1 Alignment of the fly CDT1 N-terminal fragment in the RGB cell cycle reporter (Fig2) with the human CDT1 sequence.